British Journal of Mathematics & Computer Science
20(4): 1-16, 2017, Article no.BJMCS.31355
ISSN: 2231-0851

SCIENCEDOMAIN *international*
www.sciencedomain.org

A Multi-Regions SIRS Discrete Epidemic Model With a Travel-Blocking Vicinity Optimal Control Approach on Cells

Imane Abouelkheir[1], Fadwa El Kihal[1], Mostafa Rachik[1], Omar Zakary[1*] and Ilias Elmouki[1]

[1] *Laboratory of Analysis Modeling and Simulation (LAMS), Department of Mathematics and Computer Science, Hassan II University of Casablanca, BP 7955, Sidi Othman, Casablanca, Morocco.*

Authors' contributions

All authors contributed equally and significantly to writing this paper. All authors read and approved the final manuscript.

Article Information

DOI: 10.9734/BJMCS/2017/31355
Editor(s):
(1) Kai-Long Hsiao, Taiwan Shoufu University, Taiwan.
Reviewers:
(1) D. Kiouach, Ibn Zohr University, Agadir, Morocco.
(2) Jinghai Wang, Fuzhou University, China.
(3) Wei Hsiu-Chuan, Feng Chia University, Taiwan.
(4) Orlando Jose Avila Blas, National University of Salta, Argentina.
Complete Peer review History: http://www.sciencedomain.org/review-history/17845

Original Research Article

Received: 1st January 2017
Accepted: 9th February 2017
Published: 15th February 2017

Abstract

In Susceptible-Infected-Removed-Susceptible (SIRS) compartmental models, we can suppose that a removed population has lost its immunity after being healed from an infection, and then, it moves to the susceptible compartment. In this paper, we devise a multi-regions SIRS discrete epidemic model which describes infection dynamics in regions which are connected with their neighbors by any kind of anthropological movement. We introduce controls variables into our model to show the effectiveness of movements restrictions of the infected individuals coming from the vicinity of a region we target by a control strategy we call here by the travel-blocking vicinity optima lcontrol strategy. A gridded surface of colored cells is presented to illustrate the whole domain

**Corresponding author: E-mail: zakaryma@gmail.com;*

affected by the epidemic while each cell represents a sub-domain or region. The infection is supposed starting from only one cell located in one of the borders of the surface, while the region aiming to control is supposed to be located in the center as an example to show the effectiveness of the travel-blocking vicinity optimal control approach when it is applied to a cell with 8 neighboring cells.

Keywords: Multi-regions model; SIRS epidemic model; discrete-time model; optimal control; vicinity; travel-blocking.

2010 Mathematics Subject Classification: 53C25, 83C05, 57N16.

1 Introduction

Susceptible-Infected-Removed-Susceptible (SIRS) epidemic models have been applied to situations in which it has been supposed that a removed population could move to the susceptible compartment after being healed from an infection due to the loss of its immunity. This kind of compartmental models is very useful to model the evolution of many phenomena, see as examples, subjects treated in [1],[2] and [3].

Zakary et al. have devised in 2016, a new modeling approach based on multi-regions discrete-time and continuous-time SIR models [4],[5],[6] and [7], aiming to describe the spatial-temporal evolution of epidemics which emerge in different geographical regions and to show the influence of one region on an other region via infection travel. The authors have also sought reasonable control strategies, including awareness, vaccination and travel-blocking approaches which could prevent some particular infectious diseases such as HIV/AIDS and Ebola, or epidemics and pandemics in general, from spreading more.

Here, we suppose the region we aim to control, is infected due to movements of infected people which enter only from its neighboring regions, with the hypothesis that in all regions, the removed individuals lose an amount of their immunity.

For this, we suggest here, a new modeling approach which is based on a multi-regions SIRS discrete-time epidemic model describing the spatial-temporal spread of an epidemic which emerges in a global domain of interest Ω represented by a gridded surface of colored cells which are uniform in size. These cells are supposed to be connected by movements of their populations, and they represent sub-domains of Ω or regions, noting that only one of these cells, that is targeted by our control strategy.

In [4], each region was represented by a sub-domain $(\Omega_j)_{j=1,..,p}$ while here, each region or cell is denoted by $(C_{pq})_{p,q=1,..,M}$.

For this, we assume that the epidemic can be transmitted and propagated by movements of people, from one spatial cell C_{pq}, to its neighbors or cells belonging to its vicinity. In fact, in a geographical scale relatively small, some infectious diseases such as African Swine Fever [8], Bovine Viral Diarrhoea virus [9],[10] and Foot-and-Mouth Disease [11], follow that pattern of spread, and C_{pq} can represent a farm, while in a large geographical scale such as in the case of Ebola Virus [6], SARS [12], HIV/AIDS [7],[13],[14], and ZIKA Virus [15], a cell C_{pq} can represent a city or country. Thus, the multi-cells model with the vicinity optimal control strategy can represent good approaches for infection dynamics studies regardless of the area size. In fact, the optimization criteria are chosen here in a way to restrict the movement of people coming from one or more cells

and entering other cells. Explicitly, we seek to minimize an objective function associated to C_{pq} and subject to its associated discrete-time system, with optimal control functions introduced to show the effectiveness of the travel-blocking operations followed between C_{pq} and its neighbors. V_{pq} is the vicinity set, composed by all neighboring cells of C_{pq} and which are denoted by $(C_{rs})_{r=p+k,s=q+k'}$ with $(k,k') \in \{-1,0,1\}^2$ except when $k = k' = 0$. Note also as we have mentioned before, these cells are attached just in the grid, but in reality, they are not necessarily joined together. Thus, the travel-blocking vicinity optimal control approach will show the impact of the optimal blocker controls on reducing contacts between susceptible people of the targeted cell C_{pq} and infected people coming from one cell C_{rs} or more cells from V_{pq}.

The paper is organized as follows: Section 2. presents the discrete-time multi-cells SIRS epidemic system based a colored cell modeling approach. In Section 3., we announce a theorem of necessary conditions and characterization of the sought optimal controls functions related to the travel-blocking vicinity optimal control approach. Finally, in section 4., we provide simulations of the numerical results for an example of 100 cells when an infection starts from one cell of them and which has 5 neighboring cells, while aiming to control only one cell with 8 neighboring cells.

2 The Mathematical SIRS Model

Explicitly, we consider a multi-regions discrete-time epidemic model which describes SIRS dynamics within a global domain of interest Ω which in turn is divided to M^2 regions or cells, uniform in size. In other words, $\Omega = \bigcup_{p,q=1}^{M} C_{pq}$ with C_{pq} denoting a spatial location or region.

We note that $(C_{pq})_{p,q=1,\ldots,M}$ could represent a country, a city or town, or a small domain such as neighborhoods, which belong respectively to the global domain of interest Ω which could in turn represent a part of continent or even a whole continent, a part of country or a whole country, etc.

The S-I-R populations associated to a cell C_{pq} are noted by the states $S_i^{C_{pq}}$, $I_i^{C_{pq}}$, and $R_i^{C_{pq}}$, and we note that the transition between them, is probabilistic, with probabilities being determined by the observed characteristics of specific diseases. In addition to the death, there are population movements among these three epidemiological compartments, from time unit i to time $i+1$. We assume that the susceptible individuals not yet infected but can be infected only through contacts with infected people from V_{pq} (Vicinity set or Neighborhood of a cell C_{pq}), thus, the infection transmission is assumed to occur between individuals present in a given cell C_{pq}, and is given by

$$\sum_{C_{rs} \in V_{pq}} \beta_{rs} I_i^{C_{rs}} S_i^{C_{pq}}$$

where β_{rs} is the constant proportion of adequate contacts between a susceptible from a cell C_{pq} and an infective coming from its neighbor cell $C_{rs} \in V_{pq}$ with
$V_{pq}=\left\{C_{rs} \in \Omega / r = p+k, s = q+k', (k,k') \in \{-1,0,1\}^2\right\} \setminus C_{pq}$.

SIR dynamics associated to domain or cell C_{pq} are described based on the following multi-cells discrete model

For $p, q = 1, \ldots, M$, we have

$$\begin{aligned} S_{i+1}^{C_{pq}} &= S_i^{C_{pq}} - \beta_{pq} I_i^{C_{pq}} S_i^{C_{pq}} - \sum_{C_{rs} \in V_{pq}} \beta_{rs} I_i^{C_{rs}} S_i^{C_{pq}} \\ &\quad - d S_i^{C_{pq}} + \theta R_i^{C_{pq}} \qquad (2.1) \\ I_{i+1}^{C_{pq}} &= I_i^{C_{pq}} + \beta_{pq} I_i^{C_{pq}} S_i^{C_{pq}} + \sum_{C_{rs} \in V_{pq}} \beta_{rs} I_i^{C_{rs}} S_i^{C_{pq}} \\ &\quad - (\alpha + \gamma + d) I_i^{C_{pq}} \qquad (2.2) \\ R_{i+1}^{C_{pq}} &= R_i^{C_{pq}} + \gamma I_i^{C_{pq}} - (d + \theta) R_i^{C_{pq}} \qquad (2.3) \end{aligned}$$

$i = 0, ..., N-1$

with $S_0^{C_{pq}} > 0, I_0^{C_{pq}} > 0$ and $R_0^{C_{pq}} > 0$ are the given initial conditions.

$d > 0$ is the natural death rate while $\alpha > 0$ is the death rate due to the infection, $\gamma > 0$ denotes the natural recovery rate from infection and $\theta > 0$ denotes the immunity loss rate. By assuming that is all regions are occupied by homogeneous populations, α, d and γ are considered to be the same for all cells of Ω.

3 The Travel-Blocking Vicinity Optimal Control Approach

The main goal of the travel-blocking vicinity optimal control approach is to restrict movements of infected people coming from the set V_{pq} and aiming to reach the cell C_{pq}. For this, we introduce controls $u^{pqC_{rs}}$ variables which characterize the travel-blocking strategy operation and aims to limit contacts between susceptible of the targeted cell C_{pq} and infected individuals coming from cells C_{rs} which belong to V_{pq} [16]. Then, for a given cell C_{pq} in Ω, the discrete-time system (2.1)-(2.2)-(2.3) becomes

$$\begin{aligned} S_{i+1}^{C_{pq}} &= S_i^{C_{pq}} - \beta_{pq} I_i^{C_{pq}} S_i^{C_{pq}} - \sum_{C_{rs} \in V_{pq}} u_i^{pqC_{rs}} \beta_{rs} I_i^{C_{rs}} S_i^{C_{pq}} \\ &\quad - d S_i^{C_{pq}} + \theta R_i^{C_{pq}} \qquad (3.1) \\ I_{i+1}^{C_{pq}} &= I_i^{C_{pq}} + \beta_{pq} I_i^{C_{pq}} S_i^{C_{pq}} + \sum_{C_{rs} \in V_{pq}} u_i^{pqC_{rs}} \beta_{rs} I_i^{C_{rs}} S_i^{C_{pq}} \\ &\quad - (\alpha + \gamma + d) I_i^{C_{pq}} \qquad (3.2) \\ R_{i+1}^{C_{pq}} &= R_i^{C_{pq}} + \gamma I_i^{C_{pq}} - (d + \theta) R_i^{C_{pq}} \qquad (3.3) \end{aligned}$$

$i = 0, ..., N-1$

Since our goal concerns the minimization of the number of the infected people and the cost of the vicinity optimal control approach, we consider an optimization criterion associated to cell C_{pq} and we define it by the following objective function

$$\begin{aligned} J_{pq}(u) &= A_1 I_N^{C_{pq}} \\ &\quad + \sum_{i=0}^{N-1} \left(A_1 I_i^{C_{pq}} + \sum_{C_{rs} \in V_{pq}} \frac{A_{rs}}{2} (u_i^{pqC_{rs}})^2 \right) \qquad (3.4) \end{aligned}$$

where $A_1 > 0$ and $A_{rs} > 0$ are the constant severity weights associated to the number of infected individuals and controls respectively. The control functions $u = \left(u_i^{pqC_{rs}}\right)_{C_{rs} \in V_{pq},\, i=1,\ldots,N-1}$ are

defined in the control set U_{pq} associated to the cell C_{pq}, defined by

$$\begin{aligned} U_{pq} &= \{u \ \ measurable/u^{min} \leq u_i^{pqC_{rs}} \leq u^{max},\ u^{max} < 1,\ u^{min} > 0, \\ &\quad i = 0, ..., N-1, C_{rs} \in V_{pq}\} \end{aligned} \tag{3.5}$$

Then, we seek optimal controls $u^{pqC_{rs}*}$ such that

$$J_{pq}(u^*) = min\{J_{pq}(u)/u \in U_{pq}\}$$

The sufficient conditions for the existence of optimal controls in the case of discrete-time epidemic models have been announced in [4],[5],[17] and [18].

As regards to the necessary conditions and the characterization of our discrete optimal control, we use a discrete version of Pontryagin's maximum principle [4],[5],[19].

For this, we define an Hamiltonian $\mathcal{H}$ associated to a cell C_{pq} by

$$\begin{aligned} \mathcal{H} &= A_1 I_i^{C_{pq}} + \sum_{C_{rs} \in V_{pq}} \frac{A_{rs}}{2} (u_i^{pqC_{rs}})^2 \\ &+ \zeta_{1,i+1}^{C_{pq}} \Big[S_i^{C_{pq}} - \beta_{pq} I_i^{C_{pq}} S_i^{C_{pq}} \\ &\quad - \sum_{C_{rs} \in V_{pq}} u_i^{pqC_{rs}} \beta_{rs} I_i^{C_{rs}} S_i^{C_{pq}} - d S_i^{C_{pq}} + \theta R_i^{C_{pq}} \Big] \\ &+ \zeta_{2,i+1}^{C_{pq}} \Big[I_i^{C_{pq}} + \beta_{pq} I_i^{C_{pq}} S_i^{C_{pq}} \\ &\quad + \sum_{C_{rs} \in V_{pq}} u_i^{pqC_{rs}} \beta_{rs} I_i^{C_{rs}} S_i^{C_{pq}} - (\alpha + \gamma + d) I_i^{C_{pq}} \Big] \\ &+ \zeta_{3,i+1}^{C_{pq}} \Big[R_i^{C_{pq}} + \gamma I_i^{C_{pq}} - (d + \theta) R_i^{C_{pq}} \Big] \end{aligned}$$

$i = 0, ..., N-1$
with $\zeta_{k,i}^{C_{pq}}$, $k = 1, 2, 3$, the adjoint variables associated to $S_i^{C_{pq}}$, $I_i^{C_{pq}}$ and $R_i^{C_{pq}}$ respectively, and defined based on formulations of the following theorem.

Theorem 3.1. *(Necessary Conditions and Characterization)*

Given optimal controls $u^{pqC_{rs}*}$ and solutions $S^{C_{pq}^*}, I^{C_{pq}^*}$ and $R^{C_{pq}^*}$, there exists $\zeta_{k,i}^{C_{pq}}$, $i = 0...N$, $k = 1, 2, 3$, the adjoint variables satisfying the following equations

$$\triangle \zeta_{1,i}^{C_{pq}} = -\left[(1-d)\, \zeta_{1,i+1}^{C_{pq}} + \left(\beta_{pq} I_i^{C_{pq}} + \sum_{C_{rs} \in V_{pq}} u_i^{pqC_{rs}} \beta_{rs} I_i^{C_{rs}} \right) \left(\zeta_{2,i+1}^{C_{pq}} - \zeta_{1,i+1}^{C_{pq}} \right) \right] \tag{3.6}$$

$$\begin{aligned} \triangle \zeta_{2,i}^{C_{pq}} &= -\Big[A_1 + \beta_{pq} S_i^{C_{pq}} \left(\zeta_{2,i+1}^{C_{pq}} - \zeta_{1,i+1}^{C_{pq}} \right) \\ &\quad + (1 - (\alpha + \gamma + d)) \zeta_{2,i+1}^{C_{pq}} \\ &\quad + \gamma \zeta_{3,i+1}^{C_{pq}} \Big] \end{aligned} \tag{3.7}$$

$$\triangle \zeta_{3,i}^{C_{pq}} = -\left[(1-d)\, \zeta_{3,i+1}^{C_{pq}} + \theta \left(\zeta_{1,i+1}^{C_{pq}} - \zeta_{3,i+1}^{C_{pq}} \right) \right] \tag{3.8}$$

with $\zeta_{1,N}^{C_{pq}} = 0, \zeta_{2,N}^{C_{pq}} = A_1, \zeta_{3,N}^{C_{pq}} = 0$, *are the transversality conditions.*
In addition

$$\begin{aligned} u_i^{pqC_{rs}^*} &= min\{max\{u^{min}, \\ &\quad \frac{(\zeta_{1,i+1}^{C_{pq}} - \zeta_{2,i+1}^{C_{pq}})\beta_{rs} I_i^{C_{rs}^*} S_i^{C_{pq}^*}}{A_{rs}}\}, u^{max}\}, \\ &\quad i = 0, ..., N-1 \end{aligned} \tag{3.9}$$

Proof. Using a discrete version of Pontryagin's Maximum Principle in [4],[5],[19], and setting $S^{C_{pq}} = S^{C_{pq}*}$, $I^{C_{pq}} = I^{C_{pq}*}$, $R^{C_{pq}} = R^{C_{pq}*}$ and $u^{pqC_{rs}} = u^{pqC_{rs}*}$ we obtain the following adjoint equations

$$\begin{aligned} \triangle\zeta_{1,i}^{C_{pq}} &= -\frac{\partial \mathcal{H}}{\partial S_i^{C_{pq}}} \\ &= -\left[(1-d)\,\zeta_{1,i+1}^{C_{pq}} + \left(\beta_{pq} I_i^{C_{pq}} + \sum_{C_{rs} \in V_{pq}} u_i^{pqC_{rs}} \beta_{rs} I_i^{C_{rs}}\right)\left(\zeta_{2,i+1}^{C_{pq}} - \zeta_{1,i+1}^{C_{pq}}\right)\right] \\ \triangle\zeta_{2,i}^{C_{pq}} &= -\frac{\partial \mathcal{H}}{\partial I_i^{C_{pq}}} \\ &= -\left[A_1 + \beta_{pq} S_i^{C_{pq}}\left(\zeta_{2,i+1}^{C_{pq}} - \zeta_{1,i+1}^{C_{pq}}\right) + (1 - (\alpha + \gamma + d))\,\zeta_{2,i+1}^{C_{pq}} + \gamma\zeta_{3,i+1}^{C_{pq}}\right] \\ \triangle\zeta_{3,i}^{C_{pq}} &= -\frac{\partial \mathcal{H}}{\partial R_i^{C_{pq}}} \\ &= -\left[(1-d)\,\zeta_{3,i+1}^{C_{pq}}\right] \end{aligned}$$

with $\zeta_{1,N}^{C_{pq}} = 0, \zeta_{2,N}^{C_{pq}} = A_1, \zeta_{3,N}^{C_{pq}} = 0$; the transversality conditions.

In order to obtain the optimality condition, we calculate the derivative of $\mathcal{H}$ with respect to $u_i^{pqC_{rs}}$, and we set it equal to zero

$$\frac{\partial \mathcal{H}}{\partial u_i^{pqC_{rs}}} = A_{rs} u_i^{pqC_{rs}} - \zeta_{1,i+1}^{C_{pq}} \beta_{rs} I_i^{C_{rs}} S_i^{C_{pq}} + \zeta_{2,i+1}^{C_{pq}} \beta_{rs} I_i^{C_{rs}} S_i^{C_{pq}} = 0$$

Then, we obtain

$$u_i^{pqC_{rs}} = \frac{(\zeta_{1,i+1}^{C_{pq}} - \zeta_{2,i+1}^{Cpq})\beta_{rs} I_i^{C_{rs}} S_i^{C_{pq}}}{A_{rs}}$$

By the bounds in U_{pq}, we finally obtain the characterization of the optimal controls $u_i^{pqC_{rs}^*}$ as

$$\begin{aligned} u_i^{pqC_{rs}^*} &= min\{max\{u^{min}, \\ &\quad \frac{(\zeta_{1,i+1}^{C_{pq}} - \zeta_{2,i+1}^{C_{pq}})\beta_{rs} I_i^{C_{rs}^*} S_i^{C_{pq}^*}}{A_{rs}}\}, u^{max}\}, \\ &\quad i = 0, ..., N-1, , C_{rs} \in V_{pq} \end{aligned} \tag{3.10}$$

□

4 Numerical Results and Discussions

4.1 Brief presentation

In this section, we provide numerical simulations to demonstrate our theoretical results in the case when the studied domain Ω, represent the assembly of M^2 regions or cells (cities, towns, ...). A code is written and compiled in MATLAB using data cited in Table 1. The optimality systems are solved using an iterative method where at instant i, the states $S_i^{C_{pq}}$, $I_i^{C_{pq}}$, and $R_i^{C_{pq}}$ with an initial guess, are obtained based on a progressive scheme in time, and their adjoint variables $\zeta_{l,i}^{C_{pq}}, l = 1, 2, 3$ are obtained based on a regressive scheme in time because of the transversality conditions. Afterwards, we update the optimal controls values (3.9) using the values of state and costate variables obtained in the previous steps. Finally, we execute the previous steps till a tolerance criterion is reached. In order to show the importance of our work, and without loss of generality, we consider here that $M = 10$ and then we present our numerical simulations in a 10×10 grid and which represents the global domain of interest Ω.

At the initial instant $i = 0$, susceptible people are homogeneously distributed with 50 individuals in each cell except at the upper border cell C_{15}, where we introduce 10 infected individuals and 40 susceptible ones.

In all of the figures below, the redder part of the color bars contains larger numbers of individuals while the bluer part contains the smaller numbers.

In the following, we discuss with more details, the cellular simulations we obtain, in the case when there are yet no controls.

Table 1. Parameters values of α, β, γ, d and θ associated to a cell C_{pq}, $p, q = 1, ..., M$, and which utilized for the resolution of all multi-regions discrete-time systems (2.1)-(2.2)-(2.3) and (3.1)-(3.2)-(3.3), and then leading to simulations obtained from Figure 1 to Figure 6, with the initial conditions $S_0^{C_{pq}}, I_0^{C_{pq}}$ and $R_0^{C_{pq}}$ associated to any cell C_{pq} of Ω.

$S_0^{C_{pq}}$	$I_0^{C_{pq}}$	$R_0^{C_{pq}}$	α	β	γ	d	θ
50	0	0	0.002	0.0001	0.003	0.0001	0.0002

4.2 Cellular simulations without controls

In this section, Figs 1,2 and 3. depict dynamics of the susceptible population in the case when there is yet no control strategy, followed for the prevention of the epidemic, and we note that in all these figures presented here, simulations give us an idea about the spread of the disease in the case when the epidemic starts in a cell C_{pq} with $p = 1, q = 5$ (located in the upper border of Ω). It represents the case when the vicinity set V_{pq} associated to the source cell of infection, contains 5 cells).

For instance, in Figure 1, if we suppose there are 40 susceptible people in cell C_{15} located at the upper border of Ω, and 50 in each other cell, we can see that at instant $i = 150$, the number $S^{C_{15}}$ becomes less important and takes a value close/or equal to 20, while $S^{C_{pq}}$ in cells of V_{15} take values close/or equal to 30, and as we move away from $V_{15} = \{C_{14}, C_{16}, C_{24}, C_{25}, C_{26}\}$, $S^{C_{pq}}$ remains important. At instant $i = 300$, we can observe that in most of cells, $S^{C_{pq}}$ becomes less important, taking values between 0 and 10 while in other cells, it takes values between 20 and 40 except $S^{C_{1010}}$ and its neighboring cells conserve their values in 50 since it is located far away from the source of infection. At instant $i = 450$, $S^{C_{pq}}$ becomes zero except at the corners and in most

cells at the borders of Ω because these cells have vicinity sets smaller than other cells. Finally at last instants, $S^{C_{pq}}$ converge to zero in all cells.

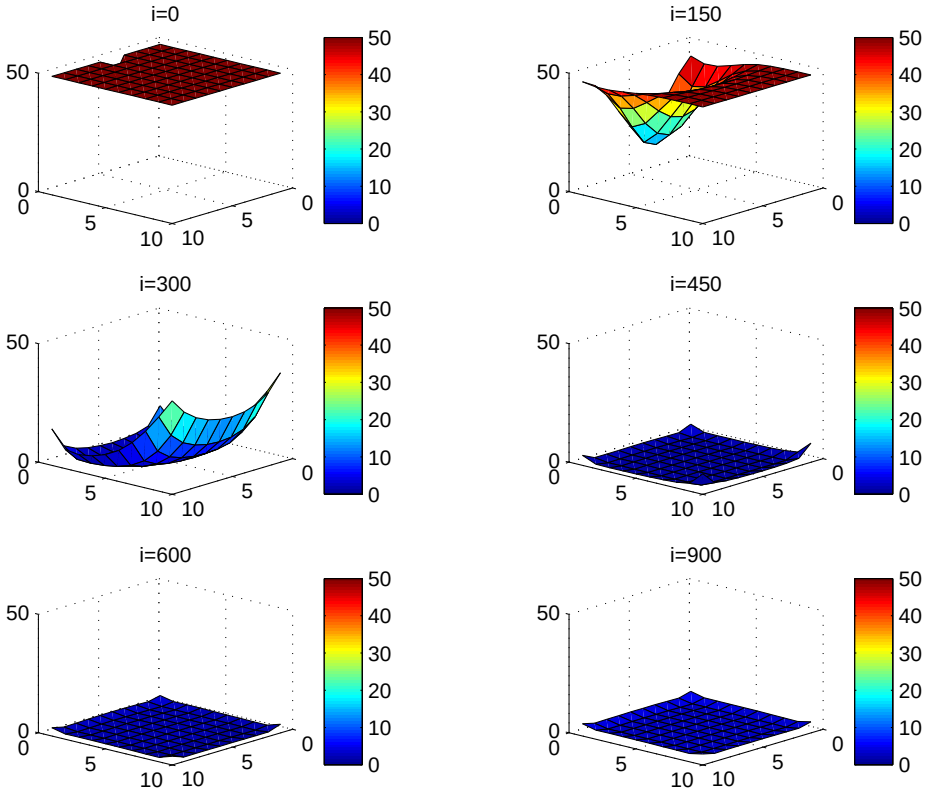

Fig. 1. $S^{C_{pq}}$ behavior in the absence of controls

Fig 2. illustrate the rapid propagation of the infection when the disease starts from cell C_{15}, and when it starts from the center of Ω respectively. In Fig 4., if we suppose there are 10 infected people in cell C_{15}, and no infection in all other cells, we observe that at instant $i = 150$, the number $I^{C_{15}}$ increases to bigger values close/or equal to 30 in C_{22}, while $I^{C_{pq}}$ in cells of V_{15} take values close/or equal to 20, and as we move away from V_{15}, $I^{C_{pq}}$ remains less important. At instant $i = 300$, we can see that in most of cells, $I^{C_{pq}}$ becomes more important, taking values between 30 and 35 in cells which are close to cells with 8 neighboring cells, while in few other cells, it takes values between 0 and 20. From these numerical results, we can deduce that once the infection arrives to the center or to the cells with 8 cells in their vicinity sets, the infection becomes more important compared to the case of the previous instant. At instant $i = 450$, $I^{C_{pq}}$ takes values close/or equal to 20 in the cell from where the epidemic has started, and 25 in V_{15} and near to it, and as we move away towards the center and further regions, infection is important with the presence of more than 30 infected individuals in each cell except the ones in the 3 opposite corners even at instant $i = 600$. In fact, at the center of Ω, the number of infected people which has increased to 35 at the previous instant, has been reduced, because once a cell becomes highly infected, it loses an important number of individuals which die or recover naturally after. All cells C_{pq} become highly infected and the number $I^{C_{pq}}$ becomes less and less important at further instants, noting that at

$i = 900$, a large number of infected individuals, has decreased because many $I^{C_{pq}}$ have died or moved to the removed compartment.

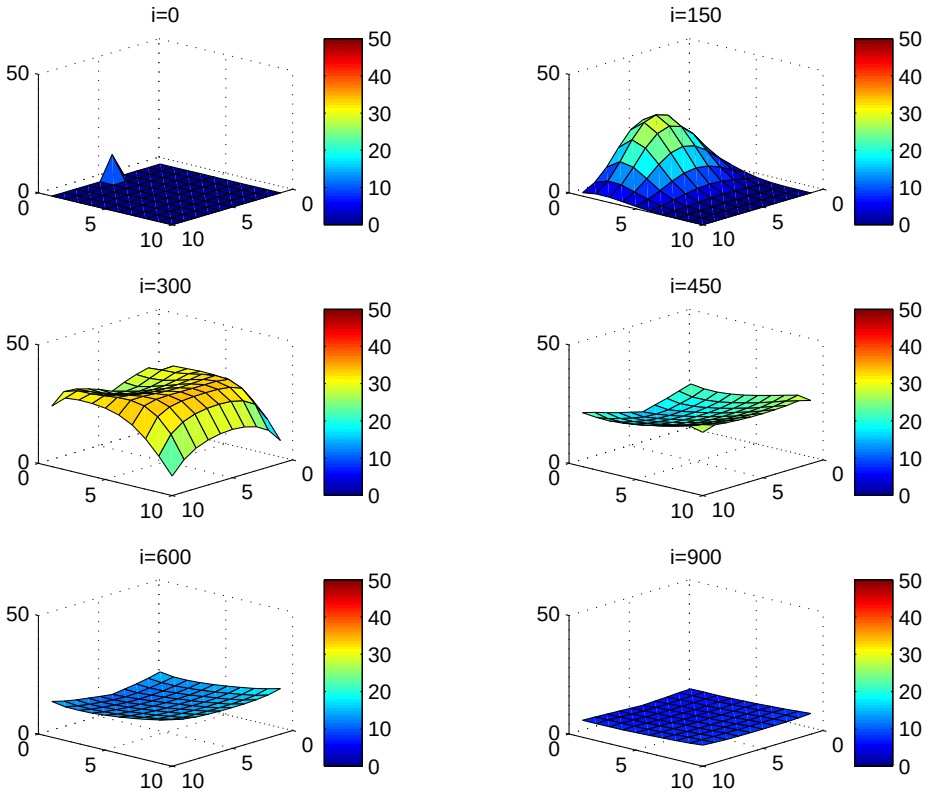

Fig. 2. $I^{C_{pq}}$ behavior in the absence of controls

As we can observe in Fig 3., when we have supposed there are 40 susceptible people in cell C_{15}, and 50 in each other cell, we can see here that simultaneously, at instant $i = 150$, the number $R^{C_{15}}$ and $R^{C_{pq}}$ in cells of V_{15} are close/or equal to only 1 or two removed people, and as we move away from V_{15}, $R^{C_{pq}}$ becomes zero. Similarly, at instant $i = 300$, the number $R^{C_{pq}}$ is not zero and takes values between 1 and 3, except for distant cells where it remains zero. At instant $i = 450$, $R^{C_{pq}}$ takes values between 3 and 5 except at the opposite 3 corners and some cells at the borders where it does not exceed 2 removed people. Finally, at further instants $R^{C_{pq}}$ converge to 5 in most cells at $i = 600$ and in all cells at $i = 900$ since as more we go forward in time, some people acquire immune responses that help them to cure naturally from the disease.

4.3 Cellular simulations with controls

Figs 4, 5 and 6. depict dynamics of the SIR populations when the travel-blocking vicinity optimal control strategy is followed.

In order to show the importance of the optimal control approach suggested in this paper, we take the example of a cell which has 8 neighboring cells, and as done in the previous part, we investigate

also here, the results obtained when the disease starts from cell C_{15} located in the upper border of Ω. As an example, we suppose that the cell we aim to control is C_{55}.

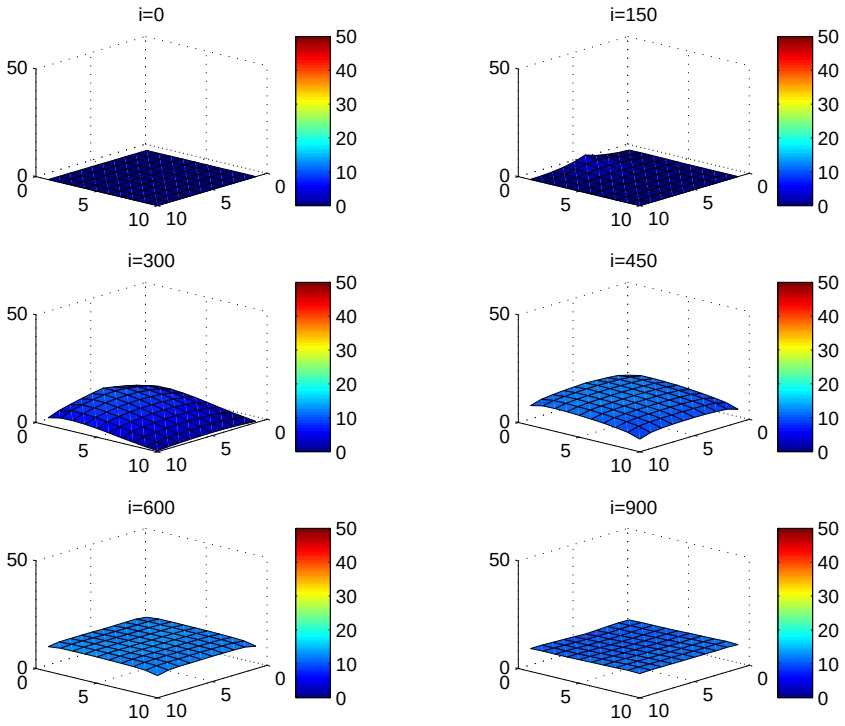

Fig. 3. $R^{C_{pq}}$ behavior in the absence of controls.

In Fig 4., as supposed also above, there are 40 susceptible people in cell C_{15}, and 50 in each other cell. We can see that at instant $i = 150$, the numbers $S^{C_{15}}$ and $S^{C_{pq}}$ are at most the same as in the case when there was no control strategy. At instant $i = 300$, we can observe that in most of cells, $S^{C_{pq}}$ becomes less important, taking values between 0 and 10 in cells that are close to V_{15}, while in other cells, and as more we move away from V_{15}, it takes values between 20 and 40. However, the controlled cell C_{55} contains 45 susceptible people. In fact, even at instant $i = 150$, the number of susceptible people in the controlled cell conserved its value in 50, which is not also exactly the same as in the case when there was yet no control strategy since in Figure 2., $S^{C_{pq}}$ has decreased more significantly. Thus, we can deduce that the travel-blocking vicinity optimal control strategy has proved its effectiveness earlier in time. At instants $i = 450, 600$ and $i = 900$, $S^{C_{pq}}$ is also the same as done before but fortunately again, we reach our goal in keeping the number $S^{C_{55}}$ close to its initial value despite some small decrease. Thus, this demonstrates that most of movements of infected people coming from the vicinity set $V^{C_{55}}$, have been restricted in final times.

In Fig 5., when the disease starts from cell C_{15}, as supposed in the section above, there are 10 infected people in cell C_{15}, and no infected in each other cell, and we can deduce that at instant $i = 150$, the numbers $I^{C_{15}}$ and $I^{C_{pq}}$ are at most the same, as shown in the absence of controls. At instant $i = 300$, we can see that in most of cells, $I^{C_{pq}}$ is similar to the case in Figure 3., and it is also more important, taking values between 20 and 30 while in other cells, it takes values between 0 and 10 as shown in the previous subsection. However, the controlled cell C_{55} is still not really infected

and contains only about one infected individual. At instant $i = 450$, $I^{C_{pq}}$ takes values around 20 in neighboring cells which belong to V_{15}, and about 30 in other cells except at the 3 opposite corners and borders of Ω. At instant $i = 600$, most cells C_{pq} begin to lose some infected individuals due to natural recovery and the number $I^{C_{pq}}$ becomes less and less important at further instants while $I^{C_{55}}$ does not exceed 2 infected individuals.

In Fig 6., when we suppose there are 40 susceptible people in cell C_{15}, and 50 others in each other cell, we can see that simultaneously, at instant $i = 150$, the number $R^{C_{15}}$ takes a value close/or equal to 5, while $R^{C_{pq}}$ in cells of V_{15} are zero, and as we move away from V_{15}, $R^{C_{pq}}$ is still zero. Similarly, at instant $i = 300$, the number $R^{C_{pq}}$ is zero at the 3 opposite corners and borders of Ω while it takes values between 1 and 3 in other cells, but $R^{C_{55}}$ is still very close to zero since very few people who have been infected there. At instant $i = 450$, $R^{C_{pq}}$ takes values between 2 and 4 except at the corners and borders while C_{55} is still not containing more than 1 or 2 people in its removed compartment. Finally at last instants, $R^{C_{pq}}$ converge to 4 at $i = 600$ in all cells except in C_{55}, and between 5 or 6 in all cells at $i = 900$ and a number of individuals close to zero in C_{55} since not many individuals have been infected to move to the removed compartment.

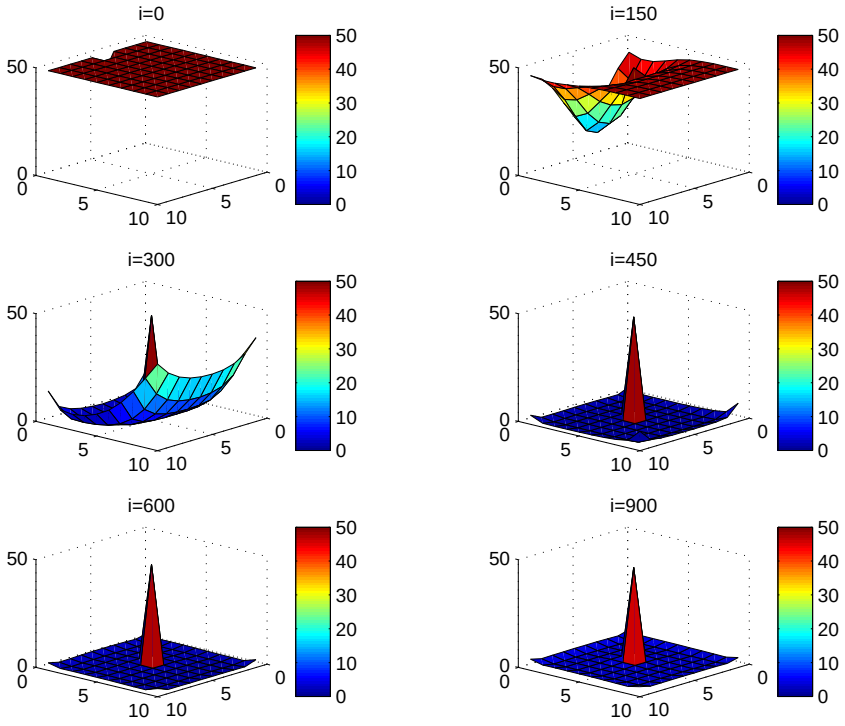

Fig. 4. C_{pq} behavior in the presence of optimal controls (3.9)

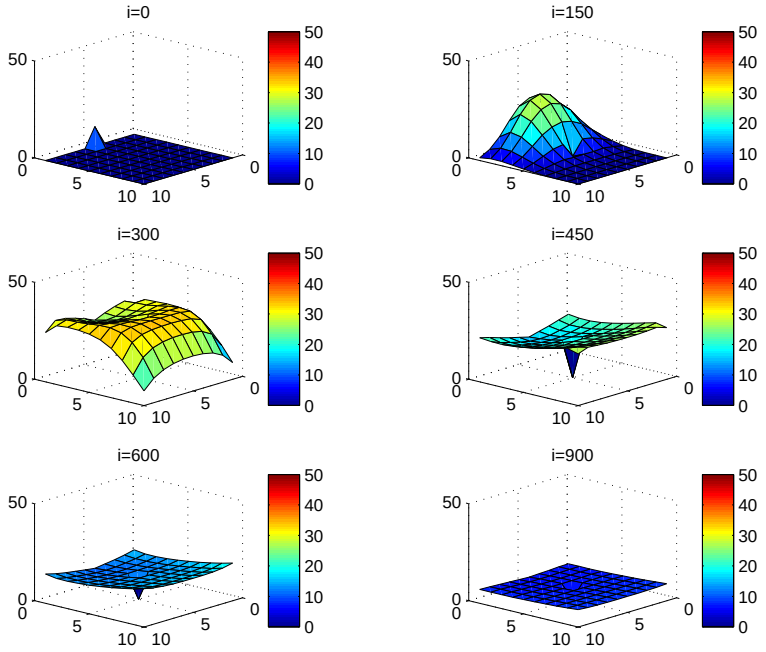

Fig. 5. $I^{C_{pq}}$ **behavior in the presence of optimal controls (3.9)**

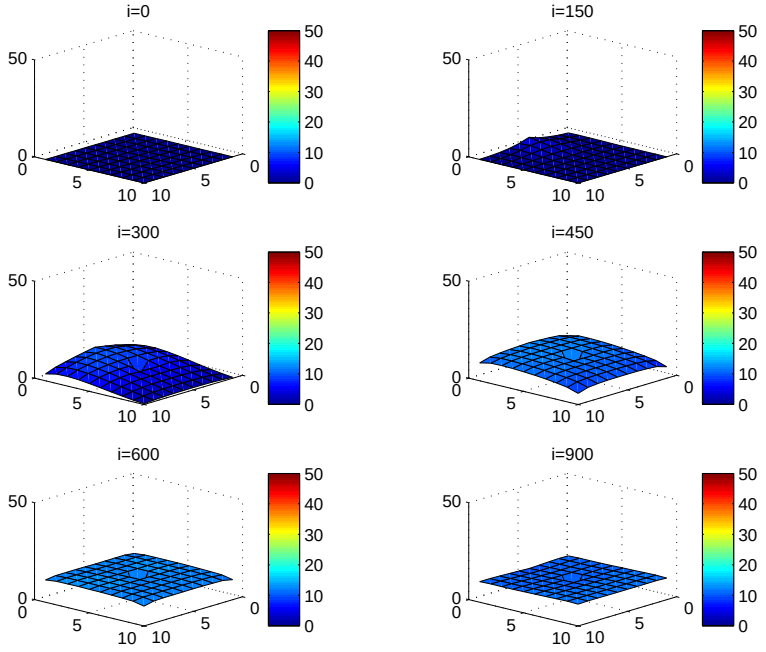

Fig. 6. $R^{C_{pq}}$ **behavior in the presence of optimal controls (3.9)**

Fig 7. depicts shapes of the optimal controls $u^{55C_{rs}}$ with $(C_{rs})_{r=5+k,s=5+k'}$, $k, k' \in \{-1, 0, 1\}$ except when $k = k' = 0$, and we mention that the optimal controls associated to the value $A_{rs} = 10^3$ are the ones utilized in simulations of Figures 4., 5. and 6. We observe that the optimal control whose severity weights are important, take smaller values.

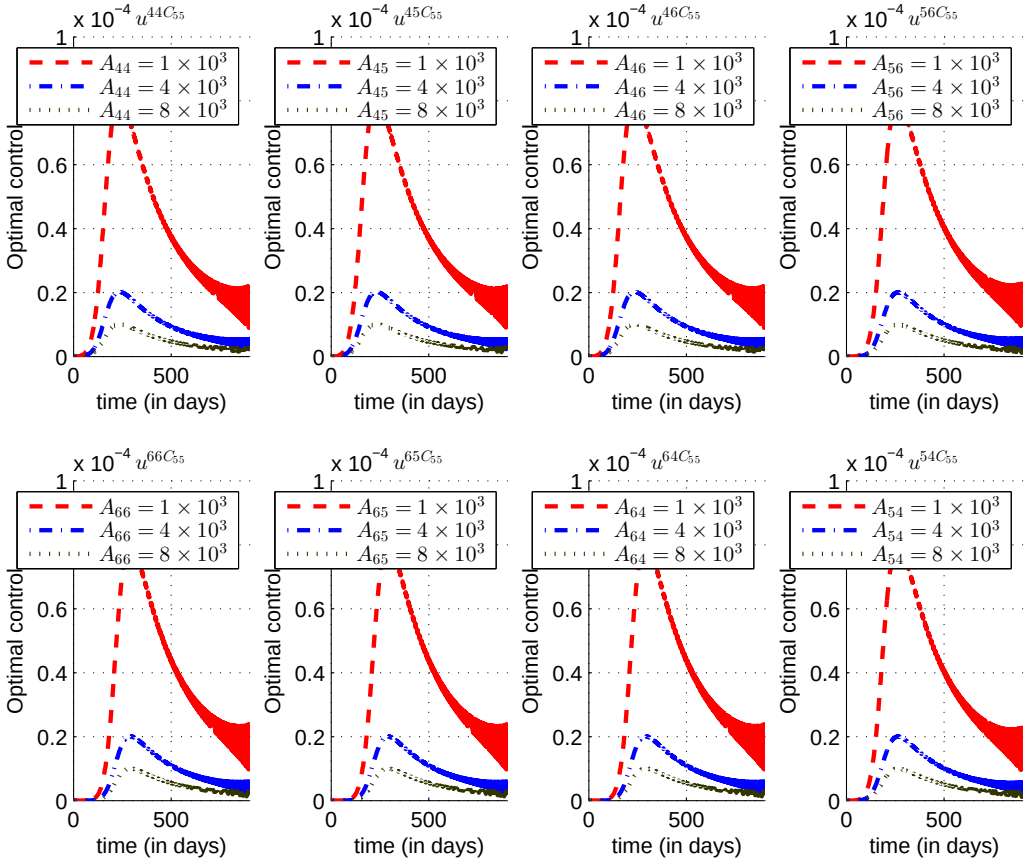

Fig. 7. The optimal controls (3.9), associated to cells which belong to V_{55}

This is a result which can be deduced directly from the characterization (3.9), and in that case, the optimal controls are more effective in reducing the number of contacts between susceptible people and infected ones, and then minimizing the number I^{pq} as we can see more clearly in Figure 8. (a), the infected population associated to the targeted cell C_{55}, take minimal values when A_{rs} is less important. The case when the optimal controls are minimal, is also beneficial for keeping the costs minimal as seen in Fig 8. (b).

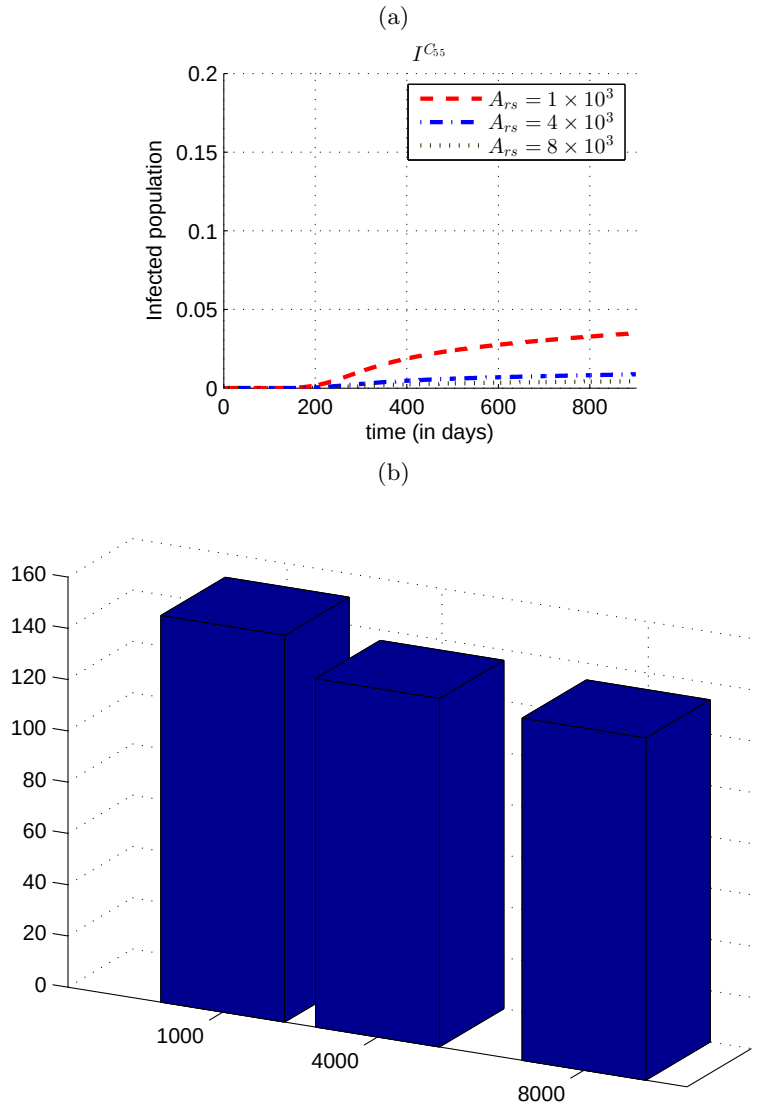

Fig. 8. (a) I^{55} behavior with respect to A_{rs}. (b) Costs with respect to A_{rs}

5 Conclusion

We devised a multi-regions SIRS discrete-time model which describes infection dynamics due to the presence of an epidemic in one region and which spreads to other regions via travel. Regions have been assembled in one gridded surface of cells where each cell represents a region, in order to exhibit the impact of infection which comes from the vicinity of a cell. In fact, by this kind of representations, we have succeeded to show the effectiveness of the travel-blocking vicinity optimal control approach when it is applied to only one cell, an then, we demonstrated that when we restrict

movements of infected people coming from the vicinity of one targeted cell, we can keep this cell safe, and without/or with no important infection. The cellular simulations in the numerical results section, have illustrated the case of 100 cells threatened by infection coming from cell called C_{15} located in the upper border of the global domain of interest Ω, while the targeted cell aiming to control, was chosen exactly in the center, called C_{55}. The travel-blocking vicinity optimal control strategy has shown its effectiveness in preventing the infection from entering the targeted cell while it was emerging in other cells where there were no controls.

Acknowledgement

Authors would like to thank all members of the Editorial baord and referees for their valuable comments. This work is supported by the Systems Theory Network (Réseau Théorie des Systèmes), and Hassan II Academy of Sciences and Technologies-Morocco.

Competing Interests

Authors have declared that no competing interests exist.

References

[1] Chaturvedi O, Masupe S, Masupe T. SIRS model for the dynamics of non-typhoidal salmonella epidemics. International Journal of Computational Engineering Research. 2013;3(10).

[2] Paladini F, Renna I, Renna L. A discrete sirs model with kicked loss of immunity and infection probability. In Journal of Physics: Conference Series, IOP Publishing. 2011;285(1);012018.

[3] Zhao H, Jiang J, Xu R, Ye Y. SIRS model of passengers panic propagation under self-organization circumstance in the subway emergency. Mathematical Problems in Engineering; 2014.

[4] Zakary O, Rachik M, Elmouki I. On the analysis of a multi-regions discrete SIR epidemic model: An optimal control approach. International Journal of Dynamics and Control. 2016;1-14.

[5] Zakary O, Rachik M, Elmouki I. A new analysis of infection dynamics: Multi-regions discrete epidemic model with an extended optimal control approach. International Journal of Dynamics and Control. 2016;1-10.

[6] Zakary, O., Rachik, M., Elmouki, I., *A multi-regional epidemic model for controlling the spread of Ebola: awareness, treatment, and travel-blocking optimal control approaches*; Mathematical Methods in the Applied Sciences (2016).

[7] Zakary O, Larrache A, Rachik M, Elmouki I. Effect of awareness programs and travel-blocking operations in the control of HIV/AIDS outbreaks: a multi-domains SIR model. Advances in Difference Equations. 2016(1):1-17.

[8] Sánchez-Vizcaíno JM, Mur L, & Martínez-López B. African swine fever: An epidemiological update. Transboundary and emerging diseases. 2012;59(s1):27-35.

[9] Fray MD, Paton DJ, Alenius S. The effects of bovine viral diarrhoea virus on cattle reproduction in relation to disease control. Animal Reproduction Science. 2000;60:615-627.

[10] Thiaucourt F, Yaya A, Wesonga H, Huebschle OJB, Tulasne JJ, Provost A. Contagious bovine pleuropneumonia: A reassessment of the efficacy of vaccines used in Africa. Annals of the New York Academy of Sciences. 2000;916(1):71-80.

[11] Grubman MJ, Baxt B. Foot-and-mouth disease. Clinical Microbiology Reviews. 2004;17(2):465-493.

[12] Afia N, Manmohan Singh, David Lucy. Numerical study of SARS epidemic model with the inclusion of diffusion in the system. Applied Mathematics and Computation. 2014;229: 480-498.

[13] Zakary O, Rachik M, Elmouki I. On the impact of awareness programs in HIV/AIDS prevention: An SIR model with optimal control. Int J Comput Appl. 2016;133(9):1-6.

[14] Samanta GP. Permanence and extinction of a nonautonomous HIV/AIDS epidemic model with distributed time delay. Nonlinear Analysis: Real World Applications. 2011;12(2):1163-1177.

[15] Chunxiao D, Tao N, Zhu Y. A mathematical model of Zika virus and its optimal control. In Control Conference (CCC), 2016 35th Chinese, TCCT. 2016; 2642-2645.

[16] Mateus ALP, Otete HE, Beck CR, Dolan GP, Nguyen-Van-Tam JS. Effectiveness of travel restrictions in the rapid containment of human influenza: A systematic review. Bulletin of the World Health Organization. 2014;92(12):868-880D.

[17] Wandi D, Hendon R, Cathey B, Lancaster E, Germick R. Discrete time optimal control applied to pest control problems. Involve, a Journal of Mathematics. 2014;7(4):479-489.

[18] Dabbs K. Optimal control in discrete pest control models. Thesis. trace.tennessee.edu; 2010.

[19] Sethi SP, Thompson GL. What is optimal control theory? Springer, US. 2000;1-22.

Peer-review history:
The peer review history for this paper can be accessed here (Please copy paste the total link in your browser address bar)
http://sciencedomain.org/review-history/17845